Optimum Design of an Electrolytic Capacitor-less Grid-tied Solar Microinverter

M. Akbari Nodehi*

*Faculty of Electrical Engineering, Shahid Rajaee Teacher Training University, Tehran,Iran; *Email: m.akbari@sru.ac.ir*

A B S T R A C T

This paper studies two types of functions for single state Solar Micro Inverter connected to a network without Electrolyte Capacitor: Continuous and Discontinues. In order to recognize the advantages of both functions and to develop the Inverter for Photovoltaic applications connected to a decentralized network; those two functions are analysed and compared.The purpose of the optimum design of these structures is a micro-inverter with the smallest possible volume to deliver maximum power to the electricity network and extensive utilization of photovoltaic energy. Using electrolyte capacitor in usual structures of Micro-Inverter circuits will lead to decrease in life span of circuits. In order to remove electrolytic capacitor, circuit analysis methods can be used for energy storage. Using the Inverter function in boundary state led to decrease in tensions imposed on Inverter's components compared to Discontinues state. Results of simulation in PSIM confirm the accuracy of analysis and designs done for 100 (W) Inverter with input DC voltage of 27 (V) and rms voltage 100 (V).

1. Introduction

Nowadays, a significant portion of required energy in industrial countries is provided by clean renewable resources. The most important factors in the reduction of fossil fuel usage demands are non-renewability, limited resources, environmental pollution and global warming due to the production of greenhouse gas. Among renewable sources like Solar, Geothermal and wind energy, direct conversion of solar energy to electrical using solar cells, has made it exclusive [1], [2].

Among different available types of solar inverters, micro-inverter technology is one of newest researches in photovoltaic systems. In the way that it converts produced electrical DC energy to AC by solar cells [1].

In this inverter, electrolyte capacitors with short life span (compared to solar plates') are used to balance between input DC power and output AC power. Short life spans of these capacitors reduce the reliability of the system. To solve this issue, small Film capacitors with long life spans can be used instead of electrolyte capacitors by making changes in the structure of micro-inverters' circuits to increase system's reliability [1], [3], [12].

Aforementioned reasons and the need for micro-inverter circuits to be compatible with various standards have caused designers to use inverters that do not contain electrolyte capacitor in their structures. Therefore, in this paper optimized design of micro-inverter without electrolyte capacitors and analysis in two functional states TM and DCM are reviewed.

Power electronics equipment which is used as a converter between solar plates produced DC energy and electricity network or feed for various loads to convert DC energy to AC consumed power, are called Solar Inverter or Micro-inverter.

Available technology in a different context as stages of energy conversion from DC to AC is classified to 1- single state 2- multi-state [4], [5], [11].

According to Figure.1 which depicts diagram block of single state solar inverter, output AC power is pulsatory and the input power is constant; this issue led to unbalanced input and output powers. Equation (1) shows the balance of solar inverter power:

$$P_{out} = v_{grid} \times i_{out} = \frac{1}{2} V_m I_m (1 - \cos(2\omega_o t))$$ (1)

I_m and V_m are network current and the voltage while P_{out} is instantaneous output power.
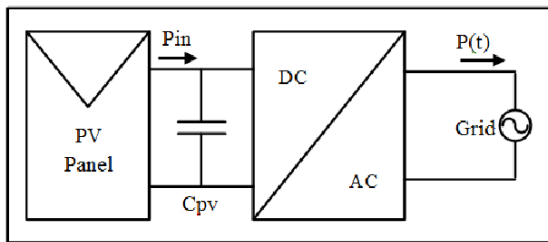

Figure 1. Schematic single stage microinverter Changes in output along with input power is shown in Figure.2.

In conventional solar inverters, in order to keep the balance between input and output powers, electrolyte capacitors are used to store energy which has shorter life span compared to solar plates, especially at the high temperatures causing system reliability to reduce.
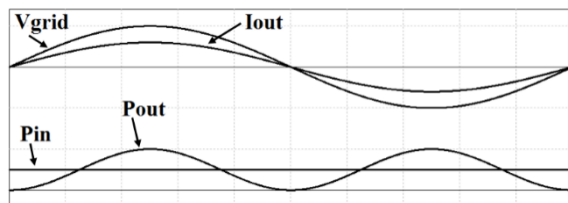

Figure 2. Description decoupling DC and AC power

In order to increase the reliability of photovoltaic systems, film capacitors with longer life span but less capacity are used instead of electrolyte capacitors. For this purpose, required energy for the circuit should be stored in a part of it so can be used when necessary. It can be expressed as this storage is directly linked to input and output power; in the way that when input power amount is more than output, excessive energy should be stored somewhere and released when input power is less than output. It can be done by a circuit called power analysis or an active filter.

In this paper which uses the idea of [6] reference, power analysis circuit consists of a capacitor and a switch, the capacitor is mainly responsible for energy storage in the circuit.

The article is as follows:
Section 2: Introducing circuit structure and used elements, Section 3: circuit analysis on the basis of DCM function, Section 4: circuit analysis on the basis of TM function, Section 5: comparison between DCM and TM functions, Section 6: simulation results, Section 7: conclusion.

2. Circuit Structure of Investigated Micro-inverter

Figure.3 depicts circuit structure of single state micro-inverter connected to the network. This structure is formed of 4 main parts: (1): photovoltaic plate (2): power analysis circuit (3): flyback inverter (4): output filter. As seen in the fig.3, the circuit consists of two Sm and Sp switches on the primary side, two Sac1 and Sac2 switches on the secondary side, and a Cp capacitor in power analysis circuits. Dm, Dac1 and Dac2 diodes prevent energy transition to opposite direction. Power analysis circuit stores required energy for balancing input and output powers.
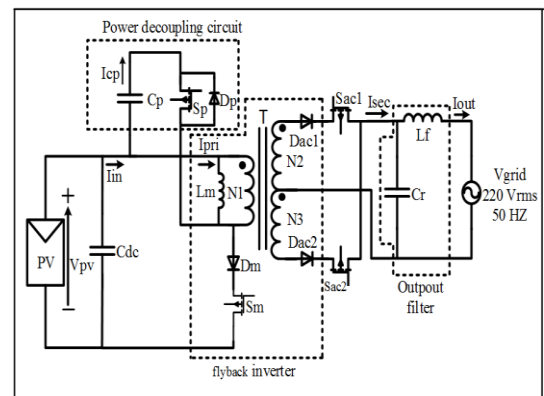

Figure 3. Microinverter structure case study [6]

3. Micro-inverter Circuit Analysis on the Basis of DCM Function

In this part, DCM function is reviewed to reach optimal design. Due to simplicity, this state is widely used for micro-inverter applications with low power [14]. Figure.4 shows the transformer's current. As can be seen, a switching period is divided into 4 intervals [6].

Stage 1 [t_0-t_1]: Sm switch is on at this stage and others off. Therefore, according to Figure.4 (a) the only pathway for input current is from primary magnetic inductor of flyback inverter:

$$I_{in}(t) = \frac{V_{pv}}{L_m} (t - t_0)$$ (2)

Where L_m and V_{pv} are self-inductance of primary coil and dc input voltage.

Stage 2 [t_1-t_2]: Sm switch is off in this interval and Sp switch is on. Figure.4 (b) shows the pathway of current in this interval. At this state, Cp capacitor current is:

$$I_{cp}=\frac{V_{cp}}{L_m}\ (t\text{-}t_1)\text{-}\ I_{in,p} \tag{3}$$

Where V_{cp} is the voltage of Cp capacitor.

Stage 3[t_2-t_3]: In this interval, stored energy on the primary side of flyback inverter is transmitted to the secondary side. Therefore, according to the polarization of network voltage, one of the switched on the secondary side is turned on. Figure.4 (c) depicts the current's pathway assuming the Sac1 switch is turned on. The current of transformer's secondary side is:

$$i_{L2}(t)=\left(\frac{N_1}{N_2}\ I_{cp,p}\right)\text{-}\left(\frac{V_m\ \sin(\omega_o t)}{L_2}\ (t\text{-}t_2)\right) \tag{4}$$

In the above relation, N_1 and N_2 are the number of turns in primary and secondary coils of the transformer.

Stage 4[t_3-t_4]: As shown in Figure.4 (d), every switch is off in this interval. At the end of this interval, the switching period is finished and circuit completed a cycle [6].

4. Micro-inverter Circuit Analysis on the Basis of TM Function

In this part, the new function of the circuit at TM state is reviewed. Contrary to DCM state, when magnetic inductor's current approaches zero at the end of switching period, it starts to charge instantly and this is an important feature of boundary state. So, switching frequency is variable in this stage [7], [8], [13].
Basic equations for analysis of TM function could be considered like DCM state. Magnetic Current Waveform of the transformer is shown in Fig.5. A switching period is divided into 3 intervals:

Stage 1[t_0-t_1]: the function of this interval is identical to DCM state and the current pathway is shown in Figure.4 (a). Equations related to this interval are:

$$I_{pv}=\frac{I_{in,p}}{2}\ D_1 \tag{5}$$

$$I_{pv}=\frac{L_m\ (I_{in,p})^2}{2\ V_{pv}\ T_s} \tag{6}$$

Current amplitude in above relation is maximum at t=t_1:

$$I_{in,p}=I_{in}(t_1)=\frac{V_{pv}}{L_m}\ D_1 T_s \tag{7}$$

$$D_1 T_s=\frac{L_m\ I_{in,p}}{V_{pv}} \tag{8}$$

Stage 2[t_1-t_2]: At t=t_1 when I_{in} is maximized, Sm switch is turned off and Sp switch is turned on according to circuit control system. The Current pathway in this interval is shown in Figure.4 (b). Equations are written below and current of Cp is:

This interval ends at t=t_2, and this is when Cp current is maximized:

$$I_{cp,p}=I_{cp}(t_2)=\frac{V_{cp}}{L_m}\ D_2\ T_s\text{-}I_{in,p} \tag{9}$$

$$D_2 T_s=\frac{L_m}{V_{cp}}\ \left(I_{cp,p}+I_{in,p}\right) \tag{10}$$

Stage 3[t_2-t_3]: switches on the primary side of inverter are off and one of secondary switches is turned on according to voltage polarity of the network, therefore stored energy in primary side of transformer is transmitted to secondary side.

$$I_{L2}(t)=\left(\frac{N_1}{N_2}\ I_{cp,p}\right)\text{-}\left(\frac{V_m}{L_2}\ (t\text{-}t_2)\right) \tag{11}$$

This interval ends at t=t_3 and I_{L2} (Isec) is zero:

$$t_3\text{-}t_2=D_3\ T_s=\frac{N_2}{N_1}\ \frac{L_m\ I_{cp,p}}{V_m} \tag{12}$$

At the end of this interval, switching period is completed.

As mentioned beforehand, inverter's function is at boundary state. According to Figure.5 it can be concluded that at boundary state a switching frequency period has two maximum ($F_{s,max}$) and minimum ($F_{s,min}$) values. As could be seen in Figure.5, switching period changes as a sine and the maximum value of switching frequency occurs at the beginning of switching period (ω_t=0) and its minimum at ($\omega_t=\frac{\pi}{2}$).

Now, ($T_{s,max}$) and ($T_{s,min}$) should be obtained by different elements' voltage and current so it can be used to achieve proper value for (L_m) and values for other elements of the circuit and also maximum and minimum switching frequency [15]. Average input power according to relation (6) is as follows:

$$P_{in}=V_{pv}\times I_{pv}=\frac{1}{2}\frac{L_m\ I_{in,p}^{\ 2}}{T_s} \tag{13}$$

And also average output power:

$$P_{out,av}=\frac{1}{2}V_m\ I_m \tag{14}$$

If relations (14) and (15) are put equal:

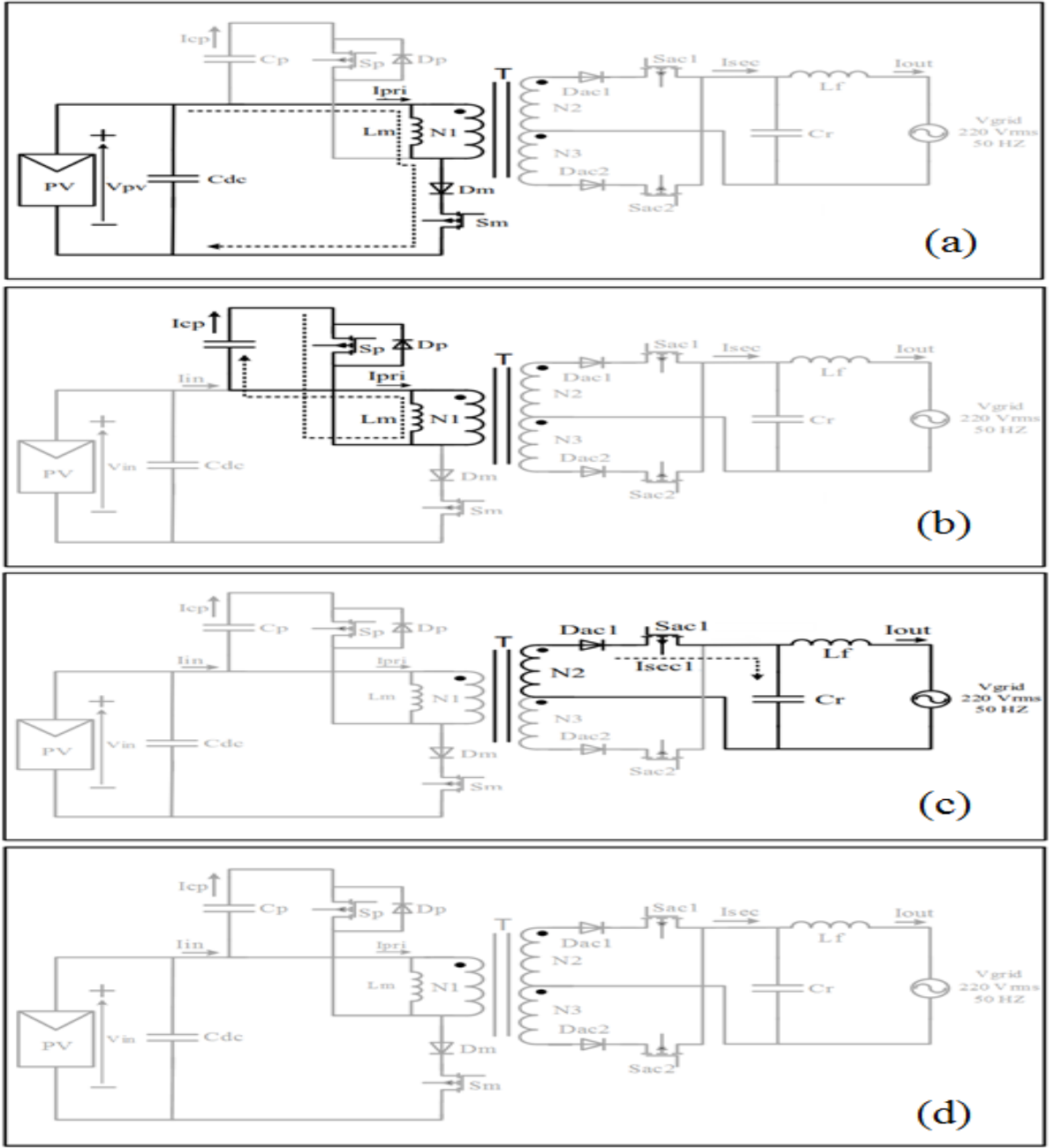$$I_{in,p}=\sqrt{\frac{V_m\ I_m\ T_s}{L_m}} \tag{15}$$

215

Figure 4. Active circuit components during DCM operation

Average value of Cp current is [6]:

$$I_{cp,p}=\sqrt{2}\ I_{in,p}\ \sin(\omega_o t) \qquad (16)$$

Accordingly inverter's function is at boundary state, sum of stages 1 to 3 intervals should apply to the equation below:

$$T_s=D_1 T_s+D_2 T_s+D_3 T_s \qquad (17)$$

From relation (8), (11) and (13):

$$T_s=\frac{L_m\ I_{in,p}}{V_{pv}}+\frac{L_m\ (I_{cp,p}+I_{in,p})}{V_{cp}}+\frac{N_2}{N_1}\frac{L_m\ I_{cp,p}}{V_m} \qquad (18)$$

With relation (17):

$$T_s=\frac{\left(\sqrt{2}\ L_m\ I_{in,p}\right)\left(\frac{V_m\ V_{cp}}{\sqrt{2}}+\left(\frac{1}{\sqrt{2}}+\sin(\omega_o t)\right)V_{pv}\ V_m+\frac{N_2}{N_1}\right)}{V_m\ V_{cp}\ V_{pv}}$$

$$(19)$$

As mentioned, the maximum switching frequency happens at the beginning of switching period, namely ($\omega_t=0$) and calculated as:

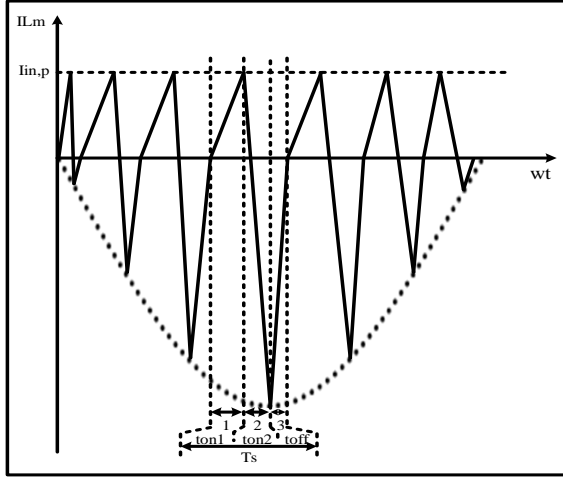$$F_{S,max}=\frac{1}{T_{s,min}}=\frac{V_{cp}\ V_{pv}}{L_m\ I_{in,p}\ (V_{cp}+V_{pv})} \qquad (20)$$

216

Figure. 5 Transformer magnetizing current wave Form in TM

Also, the minimum switching frequency happens at $(\omega_t=\frac{\pi}{2})$ calculated as:

$$F_{s,min}=\frac{1}{T_{s,max}}=$$

$$\frac{V_m\,V_{cp}\,V_{pv}}{L_m\,I_{in,p}\left((V_m\,V_{cp})+(\sqrt{2}+1)V_m V_{pv}+\frac{N_2}{N_1}\sqrt{2}\,V_{pv}\,V_{cp}\right)} \quad (21)$$

Assuming $n=\frac{N_1}{N_2}$ and definition of $\lambda=\frac{V_{pv}}{V_m}$ [9]:

$$t_{off}(t)=\frac{\lambda}{n}\sqrt{2}\,t_{on1}(t) \quad (22)$$

With relations above:

$$T_s(t)=t_{on1}+\frac{V_{pv}}{V_{cp}}(\sqrt{2}\sin(\omega_o t)+1)t_{on1}+\frac{\lambda}{n}\sqrt{2}\,t_o \quad (23)$$

$$F_{s,max}=\frac{1}{T_{s,min}}=\frac{1}{\left(1+\frac{V_{pv}}{V_{cp}}+\frac{\lambda}{n}\sqrt{2}\right)t_{on1}} \quad (24)$$

$$F_{s,min}=\frac{1}{T_{s,max}}=\frac{1}{\left(1+\frac{V_{pv}}{V_{cp}}(\sqrt{2}+1)+\frac{\lambda}{n}\sqrt{2}\right)t_{on1}} \quad (25)$$

In above relations, if $\alpha=\frac{V_{pv}}{V_{cp}}$ and $\beta=\frac{\lambda}{n}$ assumed:

$$F_{s,max}=\frac{1}{T_{s,min}}=\frac{1}{(1+\alpha+\beta\sqrt{2})t_{on1}} \quad (26)$$

$$F_{s,min}=\frac{1}{T_{s,max}}=\frac{1}{(1+\alpha(\sqrt{2}+1)+\beta\sqrt{2})t_{on1}} \quad (27)$$

Voltages values of the primary side of the inverter, Cp and solar plates curb α, λ and n parameters. According to available standards in Europe, λ values varies from 0.044-0.214 and in the USA from 0.088-0.428 [10]. The European standard is used in this paper.

Voltage value of Sm switch is obtained by:

$$V_{sm}=V_{pv}+V_{cp}\sin(2\omega_o t) \quad (28)$$

As shown, Sm switch voltage value is independent from transformer conversion ratio:

$$\frac{V_{sm,p}}{V_m}=\lambda\left(1+\frac{1}{\alpha}\right) \quad (29)$$

Above relation is independent of transformer conversion ratio and is dependent on λ and other parameters. Then values of these parameters should be chosen in a way that the maximum value of Sm switch does not excess desired value.

As shown in above Fig, with a certain λ, as a gets bigger the ratio of $(\frac{V_{sm,p}}{V_m})$ gets smaller, that means the voltage of Sm switch is decreasing. However, according to $\alpha=\frac{V_{pv}}{V_{cp}}$ relation, increasing a should lead to the decrease of Cp voltage. On the other side, if the Cp voltage is decreased, its capacity increases. As the main goal of designing this invertor is to decrease capacitor's capacity so it will be possible to use a small film capacitor with long life span instead of electrolyte capacitor with short life span, so Cp voltage can be reduced by a certain amount, and this is a limitation happens to the system.

The Voltage value of Sp switch is obtained as:

$$V_{sp}=V_{cp}\sin(2\omega_o t)+nV_m\sin(\omega_o t) \quad (30)$$

Also as shown, by using λ relations, ratio of Cp voltage and Vm can be expressed:

$$\frac{V_{sp,p}}{V_m}=\frac{\lambda}{\alpha}+n \quad (31)$$

In addition to λ, this ratio depends on the value of transformer conversion ratio (n).

According to above (31), it could be understood that for every increase in transformer conversion ratio, Cp switch voltage is also increased. So it can be concluded that there is a serious restriction in choosing proper conversion ratio. The best choice for transformer conversion ratio is at the initial area of the diagram so the maximum voltage of Sp switch will not exceed desired value.

5. Analysis and Design of Power Decoupling Circuit

As said before, to increase the reliability of inverter system, we should use small film capacitors with long life span compared to electrolyte capacitor. For this purpose, a separate circuit called power analysis circuit is used to store required energy and release it at the time of need.

Therefore, if we write the energy equation for this circuit, below relation is obtained:

$$V_{cp,max}=V_{dc,cp}+V=\sqrt{V_{dc,cp}{}^2+\frac{V_m\,I_m}{2\omega_o\,C_p}} \quad (32)$$

$$C_p=\frac{V_m\,I_m}{2\omega_o\,(V^2+2V_{dc,cp}\,V)} \quad (33)$$

$$V_{dc,cp}=\frac{1}{2}(V_{cp,max}+V_{cp,min}) \quad (34)$$

217

In the above relation, $V_{cp,max}$ is the maximum value for Cp voltage, V is the value of Cp ripple and $V_{dc,cp}$ is the average value for Cp voltage.

5.1 Comparison between DCM and TM function

After theoretical analysis, a comparison is done between two states of function. The most important function is summarized as below:

• TM function is the proper solution for high power levels.
• Control loop at TM state is more complicated. However, this loop never leads to increased expense in comparison to control loop at DCM state.
• According to different technologies used in solar plates, functions of TM state is suitable for small volumes.

6. Simulation Results and Analysis

In both functions of invertor, maximum output power is 100 (W) that uses solar plates with produced DC voltage of Vpv= 27 (V) and maximum power of 100 (W). Also, network's rms voltage is 100 (V) and the frequency is 50 (Hz). Also by using PSIM, a prototype micro-invertor which its input connected to a solar plate with maximum power of 100 (W) and 27 (V) simulated and suggests the accuracy of design relations and analyses at both states.

At TM function state, according to $\lambda = \frac{V_{pv}}{V_m}$, λ volume is calculated 0.16 which is in range of European standard [10]. According to relations (31) and (32) and also design method mentioned in previous parts, value of transformer conversion ratio at TM state is chosen n=0.5 so that Sp switch voltage do not exceed desired value. Maximum value of Sm switch voltage can calculated by relations (29) and (30). Also, Sp switch voltage is calculable by relations (31) and (32) in which one MOSFET switch with 500 (v) voltage can be used.

By choosing proper value for minimum switching frequency at $F_{s,min}$=43 (KHZ), L_m=30 (μH). Using relation (27) the maximum value of switching frequency will be $F_{s,max}$=51 (KHZ). With relations (33) and (34) C_p=40 (μf) and $V_{cp,max}$=145 (V) calculated. Finally the maximum current $I_{in,p}$=19.6 (A) and $I_{cp,p}$=27 (A). Also table 1 shows values of different voltages and currents of micro-invertor circuit at TM and DCM states. In DCM state, the transmission power in flyback converter is performed when, during a switching period, the energy stored in the transformer's primary magnetizing inductor is completely depleted and

transferred to the output. But in the TM state, the main circuit function does not change, and only the stop power transmission state will be eliminated, so one could expect that for equal power transmission in the given states the magnitude currents in the TM state will be reduced.

Figure. 6 (a) and 6 (b) respectively shows input current of invertor at DCM and TM states. Current peak at TM state decreased significantly. Also Figure.6 (c) shows magnetic inductance current at TM state which suggests circuit's proper function at TM state. Figure.6 (d) shows Cp voltage at TM state which expresses accuracy if design relations.

Table 1. Elements amounts in TM			
		TM	DCM
Input power	P_{in}	100 (W)	100 (W)
Input voltage DC	V_{pv}	27 (V)	27 (V)
Minimum switching frequency	$F_{s,min}$	43 (KHZ)	--
Maximum switching frequency	$F_{s,max}$	51 (KHZ)	--
Input capacitor DC	C_{dc}	20 (μf)	20 (μf)
Capacitor circuit power decoupling	C_p	40 (μf)	40 (μf)
Inductance magnetic	L_m	30 (μH)	25 (μH)
Maximum current	$I_{in,p}$	19.6 (A)	31.4 (A)
Maximum current capacitor power decoupling circuit	$I_{cp,p}$	27 (A)	44.4 (A)

Figure.7 (a) shows network voltage along output current before filter at TM state. Figure.7 (b) shows network voltage with output voltage after filter at TM state; as could be seen power factor is proper value of 0.997. Figure.8 shows simultaneous waveforms of input and output power and Cp voltage.

Power analysis circuit functions properly namely when input power is more than output power, capacitor stores energy and when input power is less than output power, stored energy will be released.

7. Conclusion

In this paper, two function states for solar micro-inverter connected to a decentralized network without electrolyte capacitor is reviewed. In both function states, design approach was to

achieve maximum output power. Moreover, what makes it a leading paper is using micro-invertor at TM state with minimum possible value and less tension in different components of the circuit compared to DCM state. Using a converter at the border has reduced the tensions on its components compared to a discontinuous mode.

In TM state, switching is in zero current and this causes decrease in switching losses. Another advantage of TM state is that the magnitude of the effective magnetizing current of the flyback converter has a significant reduction and this enables us to use a smaller transformator, compared to the DCM state and consequently results in the reduction of the transformer's size and core losses.
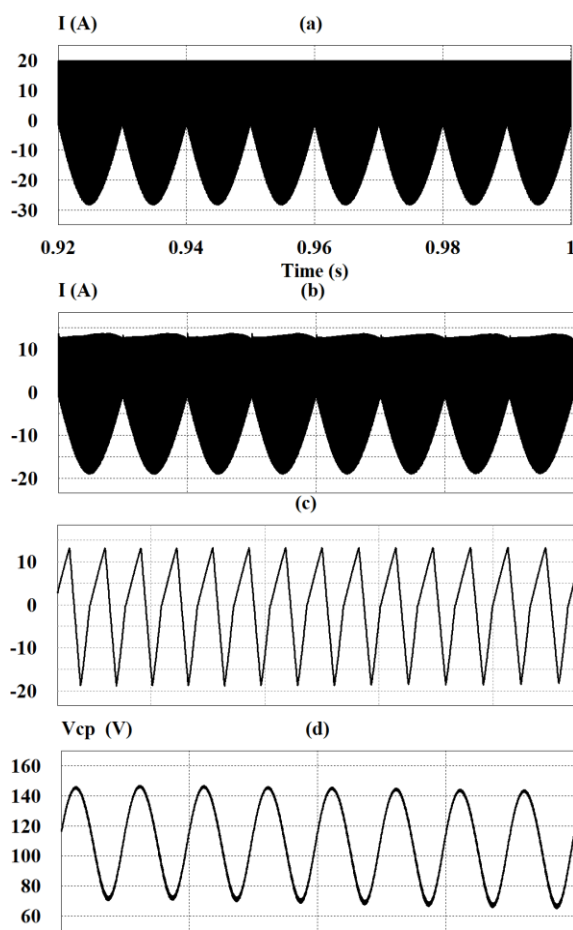
Figure. 6. (a) Input current converters in mode DCM, (b) Input current converters in mode TM, (c) magnetizing current waveform in mode TM, (d) capacitor CP voltage waveform in mode TM
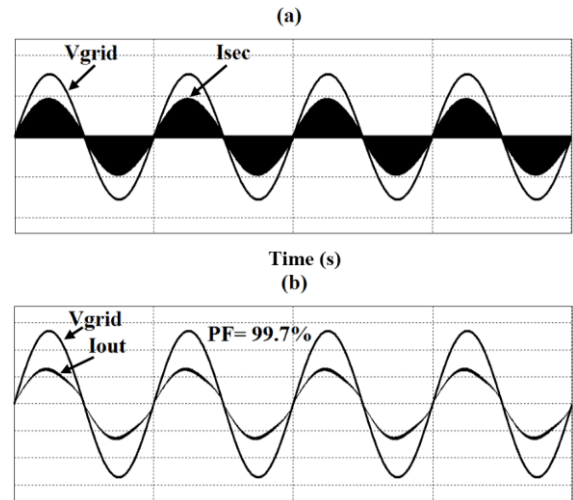
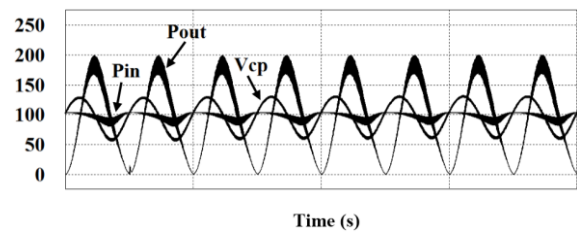Figure. 7 (a) voltage grid and pre-filter output current, (b) voltage grid and after filter output current

Figure. 8 At the same time waveforms voltage capacitor, input power, output power

References

[1] Keshani, M. and Adib, E. and Farzanehfard, H. (2017). Micro-inverter Based on Single-ended Primary-inductance Converter Topology with an Active Clamp Power Decoupling. IET Power Electronics, vol. 11, pp. 73-81.

[2] Neshaastegaran, P. and Karshenas, H. (2014). A Power Decoupling Technique for Single-Stage Micro Inverter in ac-Module Application. The 5th Power Electronics, Drive System and Technologies Conference. 120-125.

[3] Rezaei, M. (2015). Design, Implementation and Control of A High Efficiency Interleaved Flyback Micro-Inverter for Photovoltaic Applications. Thesis for receiving Ph.d degree on electrical engineering. North Carolina State University.

[4] Soeren, B. and Kjaer, J. and Pedersen, F. (2005). A Review of Single-Phase Grid-Connected Inverters for Photovoltaic Modules. IEEE Transaction on Industry Application., vol. 41, no.5, pp. 1292-1305.

[5] Quan Li, Petro Wolf. (2008). A Review of the Single Phase Photovoltaic Module Integrated Converter Topologies With Three Different DC Link Configurations. IEEE Transaction on Power Electronics., vol. 23, no. 1320-1333.

[6] Shimizo, T. and Wada, K. and Nakamura, N. (2006). Flyback-Type Single-Phase Utility Interactive Inverter With Power Pulsation Decoupling on the DC Input for an AC Photovoltaic Module System. IEEE Transaction on Power Electronics., vol. 21, no. 5.

[7] Joel Turchi, Dhaval Dalal, Patrick Wang. (2014). Power Factor Correction (pfc) Handbook, USA.

[8] Rossetto, G. and Spiazzi, P. and Tenti, Control Techniques For Power Factor Correction Converters. University of Padova- ITALY.

[9] Turki K, H. and Fadel, M. (2016). Single-Stage Grid-Connected Flyback Microinverter Operating in DCM for Photovoltaic AC Modules. International Journal of Computer Applications., vol. 138, no. 5, pp. 5-13.

[10] Kyritsis, A. and Tatakis, E. and Papanikoaou, N. (2008). Optimum Design of the Current-Source Flyback Inverter for Decentralized Grid-Connected Photovoltaic Systems. IEEE Transactions on Energy Conversion, vol. 23, no. 1, pp. 281-293.

[11] Ramprakash Kathiresan, Pritam Das, Thomas Reindl, Sanjib Kumar Panda. (2014). Purely Inductive Ripple Power Storage for Improved Lifetime in Solar Photovoltaic Micro-inverter Topology. IEEE Transaction on industry application, vol. 31, no. 0980-0985.

[12] Juan Manuel Carrasco, Jan T. Bialasiewicz, Ramón C. Portillo Guisado. (2006). Power-Electronic Systems for the Grid Integration of Renewable Energy Sources: A Survey. IEEE Transaction on Industrial Electronics, vol. 53, no. 1002-1016.

[13] Gab-Su Seo, Bo-Hyung Cho, Kyu-Chan Lee. (2012). Electrolytic Capacitor-less PV Converter for Full Lifetime Guarantee Interfaced with DC Distribution. IEEE 7th International Power Electronics and Motion Control Conference- ECCE Asia. 1235-1240.

[14] Tiesheng Yan, Jianping Xu, Fei Zhang, Jin Sha, Zheng Dong. (2013). Variable On-Time Controlled Critical Conduction Mode Flyback PFC Converter. IEEE Transactions on Industrial Electronics. pp. 1-9.

[15] Yoash Levron, Robert W. Erickson. (2015). High Weighted Efficiency in Single Phase Solar Inverters by a Variable Frequency Peak Current Controller. IEEE Transactional on Power Electronics. pp. 1-10.